J Wood Sci (1999) 45:1–9

ORIGINAL ARTICLE

Jong Su Park · Kazuo Hayashi · Kiyosei Nakamura

Trial approach to the estimation of size distribution of free water paths in the undried heartwood of softwoods by a centrifugal method*

Received: February 17, 1998 / Accepted: August 18, 1998

Abstract The size distribution of free water paths for six species of softwood was estimated from the amount of dehydrated free water under various centrifugal fields. The water permeability was evaluated simultaneously. The estimation was done by the centrifugal method, which is based on determining the balance of water potential decreased by centrifugal force and by the meniscus at small openings. The latter is determined by the radius of the capillary, the surface tension of the liquid, and the contact angle. The decrease in water potential produced by centrifugal force depends on the angular velocity, the distance from the rotational center to the dehydrated surface, and the distance inward from the dehydrated surface. We obtained the distribution of the effective radius of free water paths in undried heartwood from the distribution of the water saturation ratio in the centrifugal direction. The results showed that sugi, tsuga, and momi had peaks at around 0.50, 0.16, and 0.11 μm in the distribution curve of the free water path. The accumulation curve of the effective radius of free water paths successfully showed the water permeability. Sugi was the most permeable of the six species, and sitka spruce was the least permeable. Of the permeable species, earlywood had a larger radius than latewood.

K. Hayashi (✉)
Department of Forest Resources, College of Agriculture, Ehime University, Matsuyama 790-8566, Japan
Tel. +81-89-977-4364; Fax +81-89-946-9871
e-mail: hayashi@agr.ehime-u.ac.jp

J.S. Park
United Graduate School of Agricultural Sciences, Ehime University, Matsuyama 790-8566, Japan

K. Nakamura[1]
Department of Forest Resources, College of Agriculture, Ehime University, Matsuyama 790-8566, Japan

[1] *Present address*: Eidai Sangyo Co. Ltd., Osaka 559-0025, Japan
*This research was presented in part at the 46th and 47th annual meetings of the Japan Wood Research Socity in Kumamoto and Kochi and at the 9th Annual Meeting of Chugoku Shikoku Branch of the Japan Wood Research Socity in Tottori, April 1996, April 1997, and October 1997, respectively

Key words Centrifugal force · Capillary pressure · Undried heartwood · Distribution of radius · Permeability

Introduction

Determining the effective size distribution of free water paths is important for understanding the movement of fluid into and/or through wood. The movement of moisture in wood is closely related to permeability. Permeability is one of the most important characteristics in the field of wood processing, affecting drying, preservatives, and chemical treatment. The passageways of fluid in softwoods are mainly the cell lumen and the bordered pit pairs between tracheids. As the latter especially become a restricting factor to permeability, the correlation between permeability and wood structure has been investigated.[1–5] It is well known that permeability decreases if the torus is aspirated to the pit border or the margo is occluded by extractives. So far, the size of the free water path radius in wood has been estimated by electron microscopic investigation and gas permeability measurements.[6–8] However, these data may not provide relevant information for the field of wood drying, because predried woods were used. In the case of dried wood, it is possible that the condition of the pit changes during drying, resulting in a change in the size of the passageways.

There have been few studies to measure the permeability of undried wood. Ohgoshi et al.[9] determined the distribution of flow rates of water in never-dried hinoki and sugi sapwood by monitoring the flow of various suspensions through cross-sectional specimens. They revealed the contribution of bordered pit membrane pores to the flow through sapwood. Tremblay et al.[10] tried to establish the relation between the moisture content of wood and the water potential in desorption. In their work, they used highly compressed gas to express water from wood and then obtained the corresponding moisture content to water potential calculated from the radius producing capillary pressure. Moreover, Spolek and Plumb[11] applied the centrifugal

method to green southern pine thereby determining free water movement. They predicted the dependence of capillary pressure on the moisture content of wood using a mechanistic model that simplified the lumen geometry. They reported that capillary pressure in wood corresponded to the curvature of menisci within the lumens during the tangential movement of free water by centrifugal force. The centrifugal method was originally developed by Hassler and Brunner[12] for determining the capillary pressure in small consolidated core samples. Choong and Tesoro[13] measured ultimate dehydration at variable centrifugal forces using a short, longitudinal specimen and found that the effective pore size of softwood varied from 0.1 to 0.2 μm.

In this study, we tried to develop a new approach, called the centrifugal method, to evaluate the permeability of undried heartwood and to estimate quantitatively the distribution of the effective radius of free water paths of undried wood. The feature of this method is to measure the permeability and the effective radius from the distribution of moisture content of a comparably long specimen after centrifugal treatment. We investigated the variation in the radius of free water paths within a tree and between trees, the size distribution of free water paths for six species, and the difference of the radius of free water paths between earlywood and latewood.

Theory

This method is based on determining the average radius of free water paths from the balance of water potential decreased by centrifugal force and capillary pressure. The water potential of a substance is a measure of the capacity of that substance to work.[14] The gradient in water potential is taken as the driving force of moisture movement in wood.[10,15] Capillary pressure (ψ_c), which is the pressure decreased by the curved surface of an air–water meniscus in wood, is calculated from Eq. (1).

$$\psi_c = -\frac{2\gamma\cos\theta}{r} \tag{1}$$

where ψ_c is the capillary pressure (Pa), γ is the surface tension of water (N/m), θ is the contact angle, and r is the radius of the capillary (m). Here, minus means the pressure in the water is lower than the standard pressure of water in the wood. The absolute value of ψ_c shows the pressure differential between the water and ambient pressure.

If the water in the wood specimen is continuous, the water potential decreased by the centrifugal field is obtained as a function of the distance inward from the dehydrated surface. When r_0, l and ω are the distance from the rotational center to the dehydrated surface (m), the arbitrary distance inward from the dehydrated surface (m) and the angular velocity (s^{-1}, $2\pi n$, n: revolution per second), respectively, the centrifugal force (dF, N) acting on a narrow section, dl(m), is written as follows:

$$dF = \rho_w A dl(r_0 - l)\omega^2 \tag{2}$$

where A is the total cross-sectional area for water (m^2) and ρ_w is the water density (kg/m^3). The force acting on the water at the meniscus formed at the distance l_m from the dehydrated surface is obtained by integrating Eq. (2),

$$F = \int_0^{l_m} dF = \rho_w A\omega^2 \int_0^{l_m} (r_0 - l)dl \tag{3}$$

Evaluating integral Eq. (3),

$$F = \rho_w A\omega^2 \left(r_0 l_m - \frac{l_m^2}{2} \right) \tag{4}$$

The water potential (ψ_f) induced to this centrifugal force is shown as follows:

$$\psi_f = \frac{\rho_w}{2} l_m (2r_o - l_m)\omega^2 \tag{5}$$

where ψ_f is the water potential decreased by the centrifugal force (Pa).

The ψ_f becomes small toward the rotational center. When ψ_f becomes smaller than ψ_c, free water moves from the original site to the dehydrated surface. When ψ_f is equal to ψ_c in wood, the movement of free water stops. The ψ_f is independent of the wood structure and is determined only by experimental conditions. The movement of free water is governed by the meniscus in close relation to the free water path radius. If the movement of free water stops, the following Eq. (6) is derived from Eqs. (1) and (5) because the degree of water potential by meniscus equals that by centrifugal force.

$$r = \frac{4\gamma\cos\theta}{\rho_w l_m (2r_o - l_m)\omega^2} \tag{6}$$

where r is the radius of the free water path (m).

Figure 1 shows the relations among r, l, and rotational speed when r_o is 97×10^{-3} m. If water-saturated cells are in

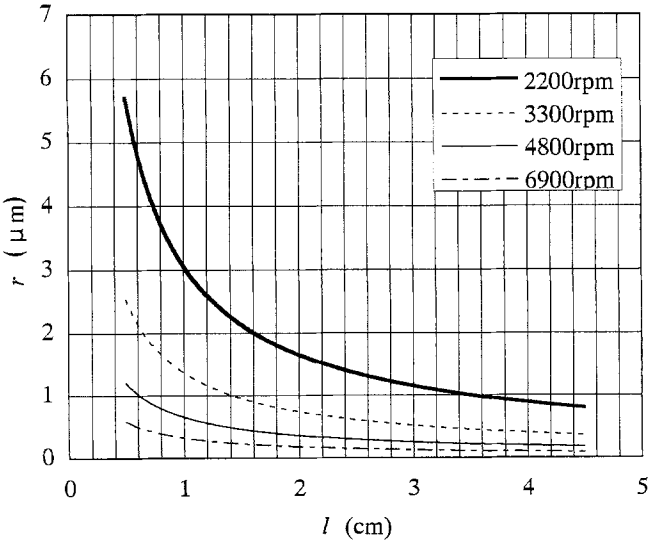

Fig. 1. Relations among the radii of free water paths (r), the arbitrary distance inward from the dehydrated surface (l), and the rotational speed (rpm) from Eq. (6) when r_o equals 97×10^{-3} m

Table 1. Physical characteristics of specimens used in this experiment

Species	Initial moisture content (%)	Mean annual ring width (cm)	Proportion of latewood (%)	Basic density (g/cm^3)
Sugi 1	47.0	0.41	15	0.28
Sugi 2	51.9	0.53	28	0.27
Tsuga	49.3	0.22	50	0.43
Momi	51.3	0.24	23	0.31
Douglas fir 1	30.0	0.32	48	0.52
Douglas fir 2	32.1	0.29	38	0.43
Sitka spruce	32.5	0.18	18	0.33
Karamatsu	31.0	0.22	41	0.43

a row, the centrifugal force in the wood increases as it nears the rotational center. By using this relation and the distribution of the water saturation ratio in the wood for various rotational speeds, we were able to obtain the distribution of the free water path radius. The water saturation ratio S, which is related to moisture content M, is calculated from Eq. (7):

$$S = \frac{\text{liquid volume}}{\text{void volume}} = \frac{M - FSP}{M_{max} - FSP} \quad (7)$$

where FSP is the fiber saturation point and M_{max} is the maximum moisture content at saturation. In this paper, FSP was 28% for all species.

Materials and methods

Green heartwoods of six species were used in this study: sugi (Japanese cedar, *Cryptomeria japonica* D. Don), tsuga (Japanese hemlock, *Tsuga sieboldii* Carr.), momi (Japanese fir, *Abies firma* Sieb. et Zucc.), Douglas fir (*Pseudotsuga menziesii* Franco), sitka spruce (*Picea sitchensis* Carr.), and karamatsu (Japanese larch, *Larix leptolepis* Gord.). The properties of the specimens are shown in Table 1. Logs of these species were cut into end matches of 10 cm long disks and then split into about $2 \times 2\,cm^2$ cross-section specimens. Specimens were then taken from the heartwood. Each specimen was saturated by immersion in distilled water under alternating vacuum and atmospheric pressure to create a row of water-saturated cells in the specimen. After the specimens were immersed in water, they were subjected to the same treatment for more than a week to ensure complete saturation. After water saturation treatment was completed, the specimen was divided into two 5 cm long samples, and lines were drawn on them to prepare thin sections. Each sample was put in an individual sample holder and placed in a well-balanced case. There were many small holes in the bottom of the sample holders, and the water was removed through the holes. Therefore, samples had no contact with the removed water.

The centrifugal apparatus Sakuma M160-IV was used for this study. The distance from the rotational center to the dehydrated surface was 9.7 cm. The rotational speed was selected at four levels from 2200 to 6900 rpm. End-matched specimens were allocated to four levels of rotational speed. The ambient temperature for the centrifugal treatment was always maintained at 10°C.

Four samples were simultaneously treated for each run. Free water was dehydrated in the longitudinal direction. The treatment time of dehydration by centrifugation was determined as the time until the weight of each sample became constant. The dehydration ratio of permeable species became nearly constant after 5 h. Some less permeable species did not show constant values, although the treatment was stopped after 5 h to maintain comparable conditions for all species. After the treatment, the samples were divided into six longitudinal sections (four sections of 1 cm thick and both end sections of 0.5 cm) at the lines drawn before.

Each section was weighed. The sections were then divided into earlywood and latewood. Each small section of the earlywood and latewood was weighed immediately; it was then resaturated to obtain the M_{max}, and oven-dried at 103° ± 2°C. The radius of the free water paths was calculated by Eq. (6) from the rotational speed, the cutting position, and the rotational radius, r_o.

The distribution of the radius of the free water path was obtained from the difference of the water saturation ratios between adjacent sections. Different centrifugal forces were applied to the samples to obtain a wide distribution of the free water path radius, which was estimated using the average values of 8 or 16 samples.

Results and discussion

Water saturation ratio

Table 2 shows an example of the water saturation ratio, S, of each section of sugi and Douglas fir after dehydration. Sections with small numbers always have a lower water saturation ratio than those with a large number, except no. 6, which had many incomplete tracheids. Section no. 1 also contains incomplete tracheids. Therefore, sections nos. 1 and 6 were not used for measurement of the water saturation ratio. The values of nos. 2–5 were used to calculate the distribution of the free water path radius. The

Table 2. Distribution of the water saturation ratio (%) after dehydration by centrifugal treatment

No. of section[a]	2200 rpm		3300 rpm		4800 rpm		6900 rpm	
	Sugi	Douglas fir	Sugi	Douglas fir	Sugi	Douglas fir	Sugi	Douglas fir
1	25.8	33.8	9.4	26.1	5.4	20.4	1.6	14.3
2	56.5	66.0	27.4	50.4	13.7	43.4	4.0	30.5
3	69.5	74.4	40.6	56.2	20.1	49.8	5.2	38.7
4	81.7	81.0	62.7	65.2	26.5	52.2	8.2	44.3
5	90.3	89.4	85.3	81.4	55.4	69.8	16.0	47.8
6	78.6	74.9	72.1	73.0	65.8	60.6	36.4	56.4

[a]The small number represents the section near the center of rotation. The distance from the center of rotation to the surface of dehydration is 97×10^{-3} m. Water saturation ratio was calculated by Eq. (7)

Table 3. Range of radius and representative value for each section

No. of section	2200 rpm		3300 rpm		4800 rpm		6900 rpm	
	Range	RV	Range	RV	Range	RV	Range	RV
2	<0.99	—	<0.44	—	<0.21	—	<0.10	—
3	0.99–1.31	1.12	0.44–0.58	0.50	0.21–0.28	0.24	0.10–0.14	0.11
4	1.31–2.05	1.59	0.58–0.91	0.70	0.28–0.43	0.33	0.14–0.21	0.16
5	2.05–5.83	3.01	0.91–2.59	1.34	0.43–1.23	0.63	0.21–0.59	0.31

RV, representative value for the radius corresponding to the average value of the centrifugal forces calculated at both ends of each section.
Results are in micrometers

calculation was based on the assumption that the free water was continuous from the meniscus to the dehydrated surface.

The procedure to obtain the distribution of radius was as follows: (1) The range of radius for each section was obtained using Eq. (6) for each rotational speed, as shown in Table 3. (2) The radius that corresponded to the average value of the centrifugal forces calculated by both ends of each section was calculated as the representative value (RV) for each section. (3) The frequency of the effective radius of free water paths was evaluated by the difference of the water saturation ratios between adjacent sections. For example, in the case of sugi, because the water saturation ratios of section nos. 2 and 3 under 2200 rpm were 56.5% and 69.5%, respectively, the frequency between 0.99 and 1.31 μm was calculated as 13.0%. Under 4800 rpm, that between 0.28 and 0.43 μm was calculated as 6.4% for sections nos. 3 and 4. The water saturation ratio for no. 2 shows the frequency of radius below the maximum radius of no. 2, corresponding to the boundary of nos. 2 and 3, because section no. 1 contains many incomplete tracheids, as mentioned above. Therefore, in this case the frequency below 0.10 μm was 4.0%. (4) The frequency value was considered to be the amount of free water held by capillary pressure calculated from the above-mentioned representative value. (5) As the thickness of each section was the same, the range of capillary radius corresponding to each section differed according to the position inward from the dehydrated surface. Therefore, the distribution of the effective radius for RV was obtained from the saturation ratio per unit range of radius. (6) To estimate the wider distribution, the range of radius calculated for each run overlapped the next one. The free water path radius estimated in this study was in the range of 0.11–3.01 μm (Table 3).

Variation of the radius of free water paths

The size variations of free water paths within and between trees were examined under various velocities. Figure 2 shows the variation in the estimated effective radius of the free water paths within trees under 3000 rpm, which corresponded to a range of 0.60–1.62 μm. Each specimen was taken from a neighboring portion separated by a distance of 4 cm. The variation in both tangential and radial directions in Douglas fir was lower than that in sugi. Douglas fir contained a large frequency below 0.53 μm, and sugi had the mode at 0.85 μm. These results indicate that sugi has a larger free water path radius than does Douglas fir.

Figure 3 shows the variation in the accumulation curves of the radius of free water paths between trees of the same species. It was also clear that Douglas fir has a smaller effective radius than sugi because the accumulation curves for Douglas fir were located further left than those for sugi. However, the variation within the same species also existed in Douglas fir.

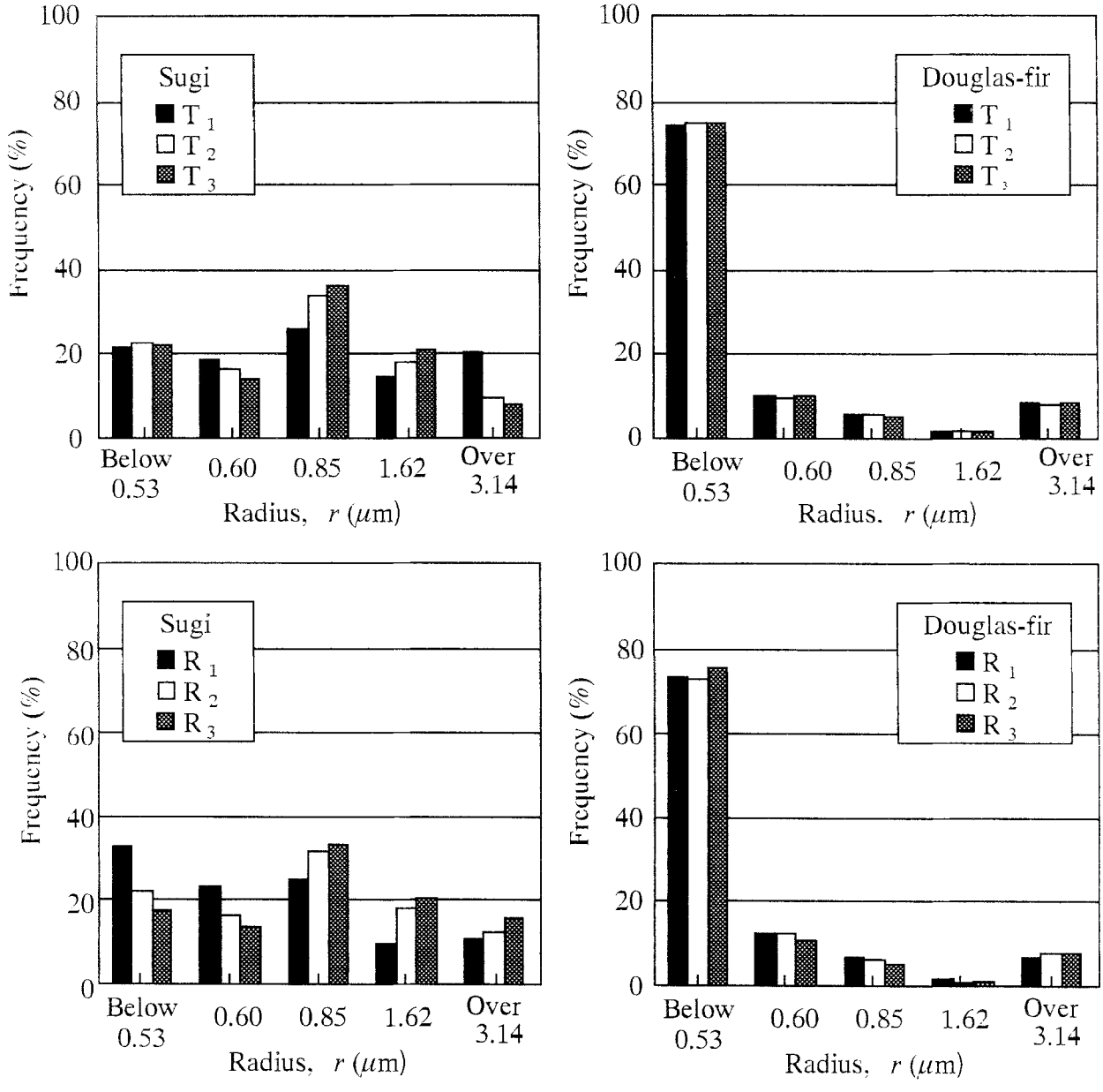

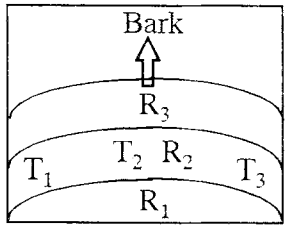

Fig. 2. Variations in the radius of free water paths within the same trees. T_1, T_2, T_3, tangential directions of specimens; R_1, R_2, R_3, radial directions of specimens

Distribution of the radius of free water paths

Figure 4 shows the accumulation and distribution curves of the radius of free water paths for sugi, tsuga, and momi, which are known as permeable species in dried conditions.[16]

Figure 5 shows those for Douglas fir, sitka spruce, and karamatsu, which are known as poorly permeable species in dried conditions.[16]

Compared to the accumulation curves, sugi shifted at the rightmost side in the six species, and so sugi was evaluated

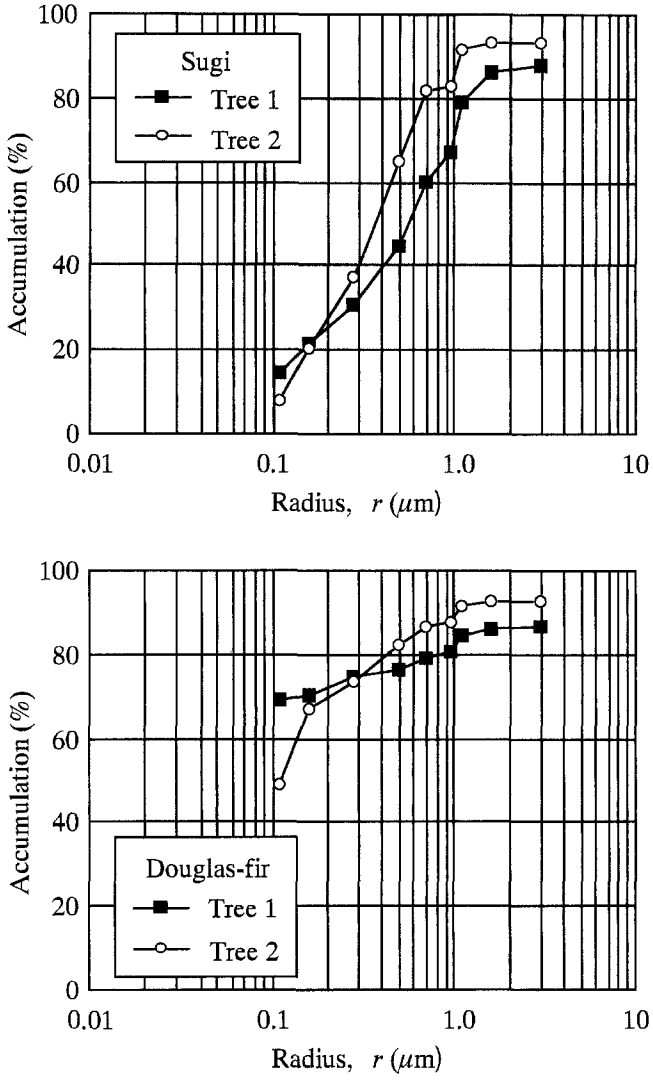

Fig. 3. Variation in accumulation curves of the radius of free water paths between trees of the same species

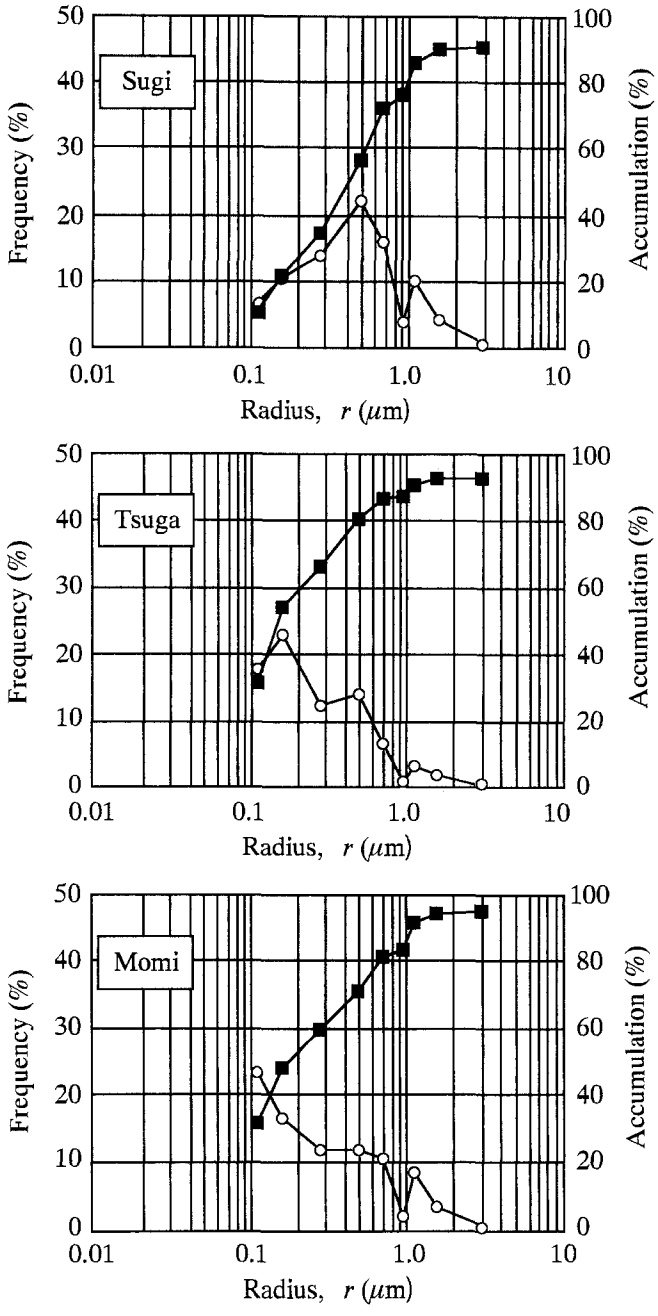

Fig. 4. Accumulation and distribution curves of the radius of free water paths for sugi, tsuga, and momi. *Circles*, frequency; *squares*, accumulation

as having the largest path system. Sugi followed momi, karamatsu, tsuga, and Douglas fir, in turn. Sitka spruce shifted at the leftmost side and was evaluated as having the smallest path system of these six species.

Table 4 shows the water saturation ratio of each species after 5 h of centrifugal treatment. The water saturation ratio was calculated as follows:

$$S = \frac{\dfrac{\sum(w_i - w_{oi})}{\sum w_{oi}} - 0.28}{\dfrac{\sum(w_{maxi} - w_{oi})}{\sum w_{oi}} - 0.28} \times 100 \qquad (8)$$

where w_{maxi}, w_i, and w_{oi} are the weight of each section at the water saturated condition after centrifugal treatment and at the oven-dried condition, respectively.

As this water saturation ratio shows the degree of water movement, it can be considered to indicate permeability. Thus, species with a low water saturation ratio could be evaluated as having good permeability. The permeability

Table 4. Water saturation ratio of each species after centrifugal treatment for 5 hours

Species	Ratio (%)			
	2200 rpm	3300 rpm	4800 rpm	6900 rpm
Sugi	67.0	49.6	31.1	11.9
Tsuga	74.2	60.9	43.4	32.2
Momi	67.3	51.3	35.7	23.9
Douglas fir	69.9	58.7	49.3	38.7
Sitka spruce	78.1	66.7	54.3	40.9
Karamatsu	59.8	50.9	37.4	29.4

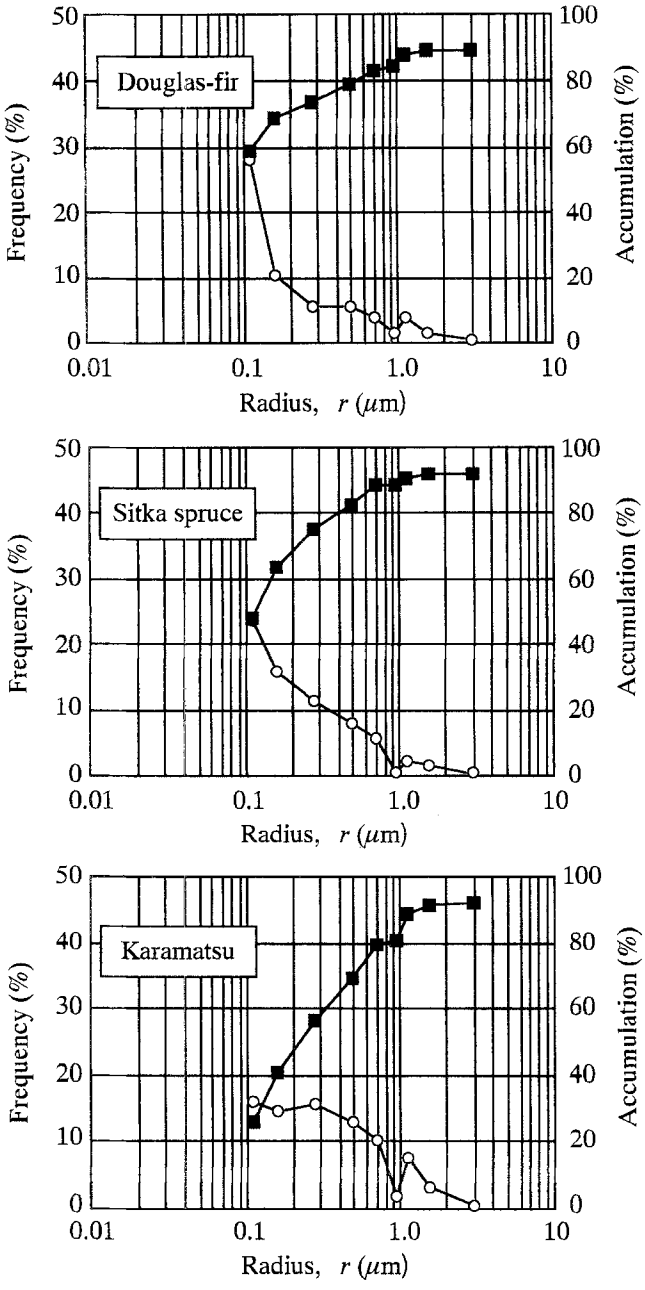

Fig. 5. Accumulation and distribution curves of the radius of free water paths for douglas fir, sitka spruce, and karamatsu. Symbols are the same as in Fig. 4

determined from dehydration coincided with the relative position of the accumulation curve of the free water path radius, indicating that the accumulation curve is a good measure of permeability. According to previous data, karamatsu is a poor permeable species. However, karamatsu showed more permeability than tsuga and was determined to have a good path system in this study. This discrepancy cannot be explained at present.

As shown in Figure 4, sugi and tsuga had clear peaks at around 0.50 and 0.16 μm, respectively. Momi did not show a clear peak in this range. It is possible that momi had a peak at 0.11 μm, judging from the small frequency below 0.10 μm, whereas other species did not have distinct peaks, as shown in Fig. 5. Douglas fir and sitka spruce had much higher frequencies below 0.10 μm. The small peak was recognized at the effective radius of 1.12 μm for all species.

There are few reports on peaks corresponding to the opening structure in wood. Sebastian et al.[7] calculated the effective pore radii using a modification of Adzumi's theory on the flow of gases through a porous wall. This calculation assumed that the longitudinal flow through the wood was governed by pit membrane openings at the overlap between the tracheids. They calculated the radii as 0.8–4.8 μm, with an average of 2.33 μm, for pit membrane openings in the heartwood of western white spruce, although they found smaller values (radius 0.66 μm) by microscopy. Comstock[6] calculated values of 0.3–1.0 μm for eastern hemlock from slip-flow measurements. Taniguchi et al.[17] measured the pore structure of dried Japanese cypress using a mercury porosimeter method and found a maximum value at a radius of 0.65 μm. They emphasized that the value of 0.65 μm obtained from the pore size distribution is in the range of pit membrane openings. Siau[18,19] mentioned that the effective radius of pit openings in softwoods probably ranges from 0.01 to 2.00 μm, depending on the species, the condition of the pits, and the method of measurement.

There is a possibility that some of the above-mentioned radii do not correspond to the inherent opening structure of wood. The peak values obtained in this study are related to the radius of the pit membrane opening. They, however, are unlikely to match openings in heartwood, where a large number of the bordered pit pairs seems to be aspirated to the pit border.

Although it is not certain whether the movement of fluid is affected by the presence of warts, it seems worthy of note that all permeable species have a warty layer and all poorly permeable species have none. According to measurements by Liese[20] the height of warts ranged from 0.5 to 1.0 μm. If warts are present on the pit border opposite the lumen, there is the possibility of incomplete pit aspiration in permeable species. It is also possible that the torus is ruptured by a constant ratio in the process of pit aspiration, which is caused by large capillary tension.

For these reasons, it seems that the peaks shown in this study for heartwood do not agree with the inherent opening structures of the wood. We suggest the possibility that the estimated water path radii are due to the incomplete pit aspiration by the presence of warts and incomplete occlusion, including rupture of the torus.

Difference of the radius of free water paths between earlywood and latewood

Figure 6 shows the accumulation curves of the effective radius of free water paths between earlywood and latewood. The accumulation curve of earlywood for sugi, tsuga, and momi is located more to the right side than with latewood. This tendency was especially clear in sugi. The result indicates that earlywood has a larger path system than latewood. However, the comparison of earlywood and late-

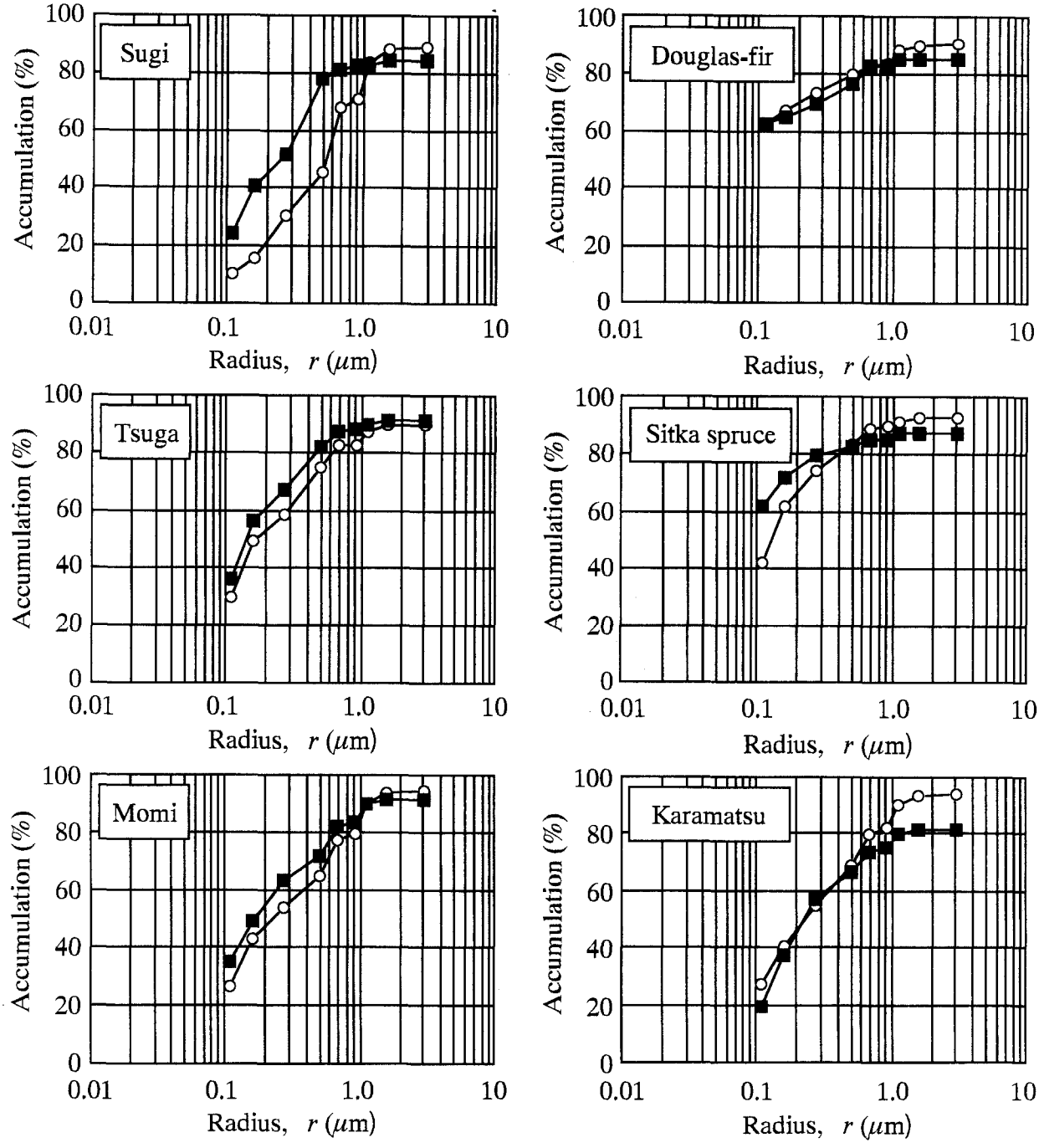

Fig. 6. Difference of accumulation curves of the radius of free water paths for earlywood and latewood. *Circles*, earlywood; *squares*, latewood

wood for Douglas fir and karamatsu showed a different accumulation curve pattern. That is, the effective radius of free water paths in latewood appeared to be larger than that in earlywood, whereas for sitka spruce there was no significant pattern difference between the accumulation curves of earlywood and latewood.

It is widely believed that latewood in dry conditions is more permeable than earlywood because pit membranes in latewood have a rigid structure resistant to the capillary force caused during drying.[19] Phillips[3] found that pit aspiration occurs gradually with loss of moisture to the fiber saturation point, and at the fiber saturation point the torii in the earlywood were almost completely aspirated to the pit borders whereas a certain portion of the latewood was not. Jinxing[21] investigated the percentage of aspirated pits for radiata pine and found that the degree of pit aspiration was about 90% for earlywood and about 20% for latewood in heartwood. Thomas[22] reported a considerable reduction of liquid flow between latewood tracheids is to be expected because of the presence of heavy incrustations. Judging from these results, latewood is not more permeable than earlywood in the undried condition. The degree of pit aspi-

ration seems to depend on the species and the conditions. In comparison to the permeable and poorly permeable species studied here, it was interesting that the effective radius of the free water paths of the undried earlywood was larger than that of the undried latewood for permeable species only.

Conclusion

The centrifugal method was used to quantitatively determine the distribution of the effective radius of the free water path. Using this method, we have obtained the following results.

1. Douglas fir was more homogeneous than sugi in the effective radius of free water paths. That is, the variation of the radius of the capillaries in Douglas fir was lower than that in sugi in both tangential and radial directions.

2. The water saturation ratio after dehydration by centrifugation was related to the relative position of the accumulation curve of the effective radius of free water paths.

3. Sugi, tsuga, and momi had peaks at around 0.50, 0.16, and 0.11μm, respectively, whereas other species did not have distinct peaks. A small peak was recognized at the effective radius of 1.12μm for all species. None of the peaks agreed with the inherent opening structure of wood. Douglas fir and sitka spruce had high frequencies in the range below 0.10μm.

4. Earlywood had a larger opening system than latewood in permeable species.

Acknowledgments This work was supported in part by financial aid from the Scientific Research Fund (no. 08456089) of the Japanese Ministry of Education, Science, and Culture.

References

1. Hart CA, Thomas RJ (1967) Mechanism of bordered pit aspiration as caused by capillarity. For Prod J 17(11):61–68
2. Liese W, Bauch J (1967) On the closure of bordered pits in conifers. Wood Sci Technol 1:1–13
3. Phillips EWJ (1933) Movement of the pit membrane in coniferous woods with special reference to preservative treatment. Forestry 7:109–120
4. Comstock GL, Côté WA Jr (1968) Factors affecting permeability and pit aspiration in coniferous sapwood. Wood Sci Technol 2:279–291
5. Comstock GL (1965) Longitudinal permeability of green eastern hemlock. For Prod J 15(10):441–449
6. Comstock GL (1967) Longitudinal permeability of wood to gases and nonswelling liquids. For Prod J 17(10):41–46
7. Sebastian LP, Côté WA Jr, Skaar C (1965) Relationship of gas phase permeability to ultrastructure of white spruce wood. For Prod J 15(9):394–404
8. Stamm AJ (1970) Maximum effective pit pore radii of the heartwood and sapwood of six softwoods as affected by drying and resoaking. Wood Fiber 1:263–269
9. Ohgoshi M, Nakato K, Sadoh T (1982) Contribution of bordered-pit membrane pores to flow through softwoods. Mokuzai Gakkaishi 28:590–595
10. Tremblay C, Cloutier A, Fortin Y (1996) Moisture content-water potential relationship of red pine sapwood above the fiber saturation point and determination of the effective pore size distribution. Wood Sci Technol 30:361–371
11. Spolek GA, Plumb OA (1981) Capillary pressure in softwoods. Wood Sci Technol 15:189–199
12. Hassler GL, Brunner E (1945) Measurement of capillary pressures in small core samples. Trans AIME 160:114–123
13. Choong ET, Tesoro FO (1989) Relationship of capillary pressure and water saturation in wood. Wood Sci Technol 23:139–150
14. Kramer PJ (1983) Water relations of plants. Academic Press, San Diego, pp 20–49
15. Siau JF (1984) Transport processes in wood. Springer-Verlag, Berlin Heidelberg New York Tokyo, pp 118–131
16. Japan Wood Preserving Association (1982) Wood preservation. Japan Wood Preserving Association, Bunkyo-shuppan, p 193
17. Taniguchi T, Harada H, Nakato K (1979) Pore structure of dry Japanese cypress (*Chamaecyparis obtusa* Endl.) by mercury porosimeter method. Mokuzai Gakkaish 25:528–534
18. Siau JF (1971) Flow in wood. Syracuse University Press, Syracuse, NY, pp 41–56
19. Siau JF (1984) Transport processes in wood. Springer-Verlag, Berlin Heidelberg New York Tokyo, pp 49–53
20. Liese W (1965) The warty layer. In: Côté WA Jr (ed) Cellular ultrastructure of woody plants. Syracuse University Press, Syracuse, pp 251–269
21. Jinxing L (1989) Distribution, size and effective aperture area of the inter-tracheid pits in the radial wall of pinus radiata tracheids. IAWA Bull 10(1):53–58
22. Thomas RJ (1969) The ultrastructure of southern pine bordered pit membranes as revealed by specialized drying techniques. Wood Fiber 1:110–123